Strong repulsive interactions in polyelectrolyte-liposome clusters close to the isoelectric point: A sign of an arrested state

F. Bordi, C. Cametti,* S. Sennato, and D. Truzzolillo
Dipartimento di Fisica, Universita' di Roma "La Sapienza," Piazzale A. Moro 2, I-00185 Rome, Italy
and INFM-CRS SOFT, Universita' di Roma La Sapienza, Rome, Italy
(Received 27 June 2007; revised manuscript received 19 September 2007; published 26 December 2007)

Charged colloidal particles whose interacting potential is governed by a short-range attraction and a long-range screened electrostatic repulsion contributions form aggregates whose shape, size, and overall charge are sensitively dependent on the balance between attraction and repulsion. In some cases, this class of colloidal systems shows an equilibrium cluster phase, where particles associate and dissociate reversibly into clusters. When the aggregation of the charged particles is induced by adding an oppositely charged polyion, very close to the isoelectric condition, the interaggregate interactions become very strong and a dynamical arrested state seems to occur. We provide some experimental evidences of this structural arrest in a colloid system composed by vesicles built up by a cationic lipid stuck together by an oppositely charged linear polyion, by means of the combined use of static and dynamic light scattering technique complemented by laser Doppler electrophoretic measurements. Our results show that the second virial coefficient, which is related to the potential of mean force between two adjacent aggregates, markedly increases in the vicinity of the isoelectric point. We interpret this increase as a print of strong interparticle interactions, yielding to a dynamical arrested state via cluster growth.

DOI: 10.1103/PhysRevE.76.061403 PACS number(s): 82.70.Dd

I. INTRODUCTION

Interactions of polyelectrolytes and oppositely charged lipids create a rich and interesting phenomenology that has recently attracted much interest, also because of a variety of implications in most disparate fields of technology as well as of more fundamental research. They range from problems in membrane biophysics and surfactant-induced DNA condensation, to technical issues of interest in the waste treatment or oil extraction (see Ref. [1], and references cited therein). In particular, cationic lipid-DNA complexes (lipoplexes) are finding increasing acceptance as preferential DNA delivery vehicles in the clinical practice of gene therapy [2–4].

When lipids are structured into spherical vesicles, their interactions with highly charged linear polyelectrolytes generate a rather unexpected phenomenology. If there is evidence that the liposome-polyelectrolyte complexes may undergo a restructuring processes, yielding large-scale superstructures [5–7], it has been also shown that, in appropriate conditions, the polyion-decorated liposomes (pd-liposomes) aggregate in clusters where the single vesicles maintain their individuality [8]. Moreover, this system is characterized by two peculiar effects, known as reentrant condensation and charge inversion. As a matter of fact, at a fixed liposome concentration and with the subsequent increasing of the polyelectrolyte concentration (with the increase of the polyelectrolyte-lipid molar ratio ξ), the system undergoes a condensation effect (formation of clusters of pd-liposomes). Such condensation is reentrant, meaning that the size of the clusters increases with ξ, reaches a maximum and then decreases again, approximately to their initial value. In correspondence with the maximum of the condensation, the aggregates change the absolute value of their neat electrical charge (charge inversion).

The observed phenomenology suggests that these systems belong to the class of colloids characterized by long-range electrostatic repulsions and short-range attractions [9–11], but with a distinctive tract that, in this case, both the repulsion and the attraction share a similar electrostatic nature [8].

In some cases, colloidal systems, belonging to this class, show an equilibrium cluster phase, where the primary particles associate and dissociate reversibly within the clusters [9,12–16], and where the shape and size of the aggregates are sensitively dependent on the balance between attraction and repulsion [8,9,15,17–19].

In a series of recent works [8,11,20,21], we have shown that, also in the case of pd-liposome suspensions, a cluster phase is observed in a range of the polyion-liposome concentration ratio ξ across the point of charge inversion (isoelectric point). Although some evidences about the possibility that the observed aggregation could be reversible has been reported [11], the presence of a polar solvent like water, makes it difficult to justify the formation of the clusters in terms of a reversible mechanism, where the aggregate sizes would be somehow governed by the screened electrostatic repulsion between the primary particles [11]. Intuitively, this mechanism would require the repulsions to occur on a length scale of the order of the aggregate size. However, in aqueous solvents, the screening length for electrostatic interactions is much smaller than the aggregate size (in our case much smaller than the primary particle size, that is $\approx$100 nm), at any practical ionic concentration [16]. However, the maximum aggregation, reached when the primary particles have a minimum neat charge, indicates that the aggregation should be attributed to a balance between electrostatic repulsions and some short-range attractions. The occurrence of this attractive interaction is due to the correlated adsorption of

*cesare.cametti@roma1.infn.it

polyions at the liposome surface. This conclusion is suggested by the observation that the reentrant condensation tends to disappear when, to induce the clusterization process, shorter and shorter polyelectrolyte chains are employed, so that a more and more uniform distribution of charge onto the adsorbed layer is achieved [22])

Briefly, a qualitative picture of the processes that lead to the aggregation could be sketched as follows. When linear polyelectrolytes are added to a suspension of oppositely charged liposomes, being the huge surface available to the adsorption finely distributed within the whole volume of the suspension, the polyion chains rapidly adsorb at the liposome surface [20,21,23–25]. However, repelling one another, the charged chains reconfigure themselves at the liposome surface in more or less ordered patterns, to gain some energy [26]. As an example of this mechanism, DNA adsorbed on planar lipid cationic bilayers [27–29] easily forms densely packed layers, where the chains lie flat on the surface and are locally aligned. This lateral adsorbed polyion correlation produces both the overcharging effect and the appearance of a short-range attractive potential between the different polyion-decorated liposomes (pd-liposomes). With the increase of the polyion/liposome concentration ratio ξ, the increasing number of adsorbed polyelectrolytes at the liposome surface progressively neutralizes the neat charge of the pd-liposome surface. However, depending on the relative size and charge density of the polyions and of the liposomes, polyion chains may continue to adsorb even beyond the neutralization point, so that the sign of the net charge of the whole assembly is reverted. In other words, more polyions than needed for neutralizing its original charge are adsorbed at the liposome surface. This phenomenon, described as a possible "giant charge inversion" in mixtures of oppositely charged macroions [26,30,31], has been recently shown to occur in polyion-charged liposome systems by means of small-angle neutron scattering experiments [32].

There is increasing evidence, both from experiments [33–37] and numerical simulations [38–41], that, in the presence of poly-valent counterions, a short-range attraction can be observed between like-charged macroions. Despite the great theoretical effort (see, for example, Refs. [42,43] and literature cited therein), a complete description of this counterintuitive interaction is still lacking. There is, however, a general consensus in pointing out the role that electrostatic correlations play in the mechanism of the like-charge attraction. Briefly, the origin of attraction could be traced back to the nonhomogeneous distribution of polyions which, repelling one another, form structures at the particle surface that present some degrees of a short-range order and can be treated as Wigner crystals. The conformation of these structures is sensitively dependent on the relative size of polyions and macroions, on their valences and on their electrical charge density. However, being similar, i.e., showing, on the average, an identical periodicity, they can form on different corresponding particles, interlocking patterns. Keeping this qualitative picture in mind, it is possible to understand how a short-range attraction can then arise when a "counterion domain" on one particle corresponds to a "counterion-free domain" on the other particle. In a more quantitative way, it has been shown that an attraction can arise between two like-charged surfaces immersed in an electrolyte from the nonuniform distribution of the charge ("charge patch" attraction [44,45] and recently [46]). This mechanism has been already invoked to explain the effect of different polyelectrolytes in inducing aggregation in different colloidal particle systems [36,37].

Interestingly, in several colloidal systems characterized by the simultaneous presence of short-range attraction and long-range repulsion, the colloidal cluster phase, for appropriate tuning of the external control parameters, evolves towards an arrested state [13–15,47].

In this paper, we present some experimental evidences that also the dynamics of the cluster phase, resulting when charged liposomes are glued together by oppositely charged linear polyions, is, in the vicinity of the isoelectric point, dominated by the strong repulsions between the aggregates, possibly yielding to an arrested state.

Recent numerical [48] and experimental [15] studies suggest that the dynamical arrest observed in these colloidal systems may be connected to a percolation process. On the other hand, simulations of the ground-state configuration of clusters of different sizes suggest that, when the cluster size exceeds the electrostatic screening length k^{-1}, the shape of the aggregates changes from spherical to linear [17]. In this case, the dynamic arrest would proceed via a glass transition mechanism [49]. In other words, the arrest transition would not occur because of the formation of a bonded network (percolation), but because elongated clusters would become confined by the repulsions created by themselves (nonpercolating arrested state) [49]. The clusters (as opposed to the primary particles) are hence trapped within repulsive cages generated by the long-range repulsion. This mechanism is known from the glass transition of Yukawa particles [50], where this process yields a Wigner glass that shows an aging behavior [51].

In this work, by means of combined static and dynamic light scattering and electrophoretic mobility measurements, we have characterized the cluster-cluster interactions between pd-liposome aggregates at varying polyelectrolyte-liposome molar ratio ξ, in a wide range across the isoelectric point, both in the presence and in the absence of a simple added salt (NaCl). We have observed the occurrence of strong repulsive interactions between these aggregates that may represent the prerequisite for the appearance, also in this particular system, of an arrested state. This characteristic opens further interesting opportunities for investigating the mechanisms of gelation in a colloidal system. In fact, contrarily to what is generally accepted as the necessary ingredients for the existence of both a stable aggregation and strong repulsions between the aggregates [i.e., a screened electrostatic interaction and an attractive force that originates from nonelectrostatic effects (depletion, for example)], in our case, the attractive interaction simply stems from the nonuniform distribution of the charges at the surface of the primary particles. Interestingly, in this system, the formation of a long-lived cluster phase seems to be attributed to a stabilization mechanism which is different from the "kinetic" stabilization mechanism usually invoked to explain the interruption of diffusion limited cluster aggregation (DLCA) phenomena.

In this paper, we propose for this system a different justification of the metastable phase, based on a recent model

developed by Velegol and Thwar [46] to describe the effect of a nonuniform surface charge in the colloidal interactions. Our findings suggest that the behavior of the colloidal system described in this work could be paradigmatic of a whole class of colloids characterized both by high values and by a strong nonuniformity of the electrical charge density at the particle surface.

II. EXPERIMENTAL

A. Material and liposome characterization

Liposomes were built up with 1,2-dioleoyl-3-trimethyl ammonium propane (DOTAP), a cationic lipid widely employed in DNA transfection protocols. DOTAP was purchased from Avanti Polar Lipids (Alabaster, AL) and used without further purification. The anionic polyelectrolyte employed to induce liposome aggregation was poly(acrylate) sodium salt (NaPA), a highly charged, flexible polyion with a simple chemical monomer structure $[-CH_2-CH(CO_2Na)-]$. NaPA was purchased from Polysciences, Inc., (Warrington, PA) as 0.25 (wt./wt.) solution in water, with a nominal molecular weight of 60 kDa. For all the preparations, MilliQ grade deionized water (Millipore, Billerica, MA) was employed.

Unilamellar liposomes were prepared by standard lipid film hydration method. In short, the lipid was dissolved in chloroform-methanol (1:1 vol/vol) at a concentration of 10 mg/ml. After solvent evaporation, the dried lipid film was hydrated with deionized water (electrical conductivity less than 10^{-6} mho/cm, at room temperature) at a temperature of 25 °C (well above the main phase transition temperature of DOTAP, $T_f \simeq 0$ °C). In order to form unilamellar vesicles, the lipid solution was sonicated at a temperature of 25 °C for 1 h at a pulsed power mode until the solution appeared optically transparent in white light. The solution was then filtered through a Millipore polycarbonate filter 0.45 μm in size.

Liposome size and size distribution were obtained from dynamic light scattering measurements. After sonication, liposomes have an average diameter of 80±5 nm (intensity-averaged size distribution [8]) with a moderate polydispersity of about 0.2, as expected for a rather homogeneous particle suspension.

The pH of the suspensions was checked for each sample and was found to remain constant to about the value of pH $\simeq$6.2. All the experiments were carried out at the temperature of 25.0±0.2 °C and each series was repeated several times to check reproducibility.

B. Polyion-induced liposome aggregation

The formation of the polyion-liposome complex was promoted by adding 250 μl of polyion solution (prepared at an appropriate concentration) to an equal volume of liposome suspension, in a single mixing step, this mixing order being kept fixed in all the experiments. In each sample investigated, the lipid concentration was maintained constant to the value C_L=0.6 mg/ml, corresponding to a final liposome volume fraction Φ of approximately 2.5×10^{-3}. By varying the polyelectrolyte concentration in an interval from 0.05 to 0.10 mg/ml, the whole range of polyelectrolyte/liposome charge ratios in the vicinity of the isoelectric condition, where the reentrant condensation occurs, was thoroughly explored.

In the systems investigated, the presence of very large aggregates often makes light scattering based experiments partially nonreproducible. Since large particles mainly scatter in the forward direction, the effects of these large aggregates can be greatly reduced by using backscattering detection technique. While this is only an advantage in dynamic light scattering, in static light scattering experiments, the use of a fixed angle backscattering geometry entails the disadvantage that the particle form factor cannot be obtained by using a Zimm plot [52]. Nevertheless, we chose a backscattering approach also for static light scattering experiment, to take advantage of using the same experimental setup (Malvern Zetamaster) for simultaneous measurements, exactly on the same sample, of the dynamic (the average hydrodynamic radius of the particles) and static light scattering (the "apparent" molecular weight and the second virial coefficient), and of the electrophoretic mobility (the ζ potential and/or the surface charge density of the aggregates), minimizing in this way possible spurious effects related to the time evolution of the samples. For this study, we employed a Malvern Zetamaster apparatus, equipped with a 5 mW HeNe laser and a backscattering (173°) optical fiber probe.

C. Dynamic light scattering

In the self-beating mode of the dynamic light scattering, the measured photoelectron count autocorrelation function $G^{(2)}(q,\tau)$ has the form

$$G^{(2)}(q,\tau) = A[1 + b|g^{(1)}(q,\tau)|^2], \tag{1}$$

where $g^{(1)}(q,\tau)$ is the first-order correlation function of the scattered electric field, τ the delay time, $A=N_s\langle N\rangle$ the baseline, with N_s the total number of samples and $\langle N\rangle$ the mean count per sample, b a spatial coherence factor depending on the experimental setup and on the scattering intensity [53], and q is the scattering wave vector given by $q=\frac{4\pi n}{\lambda}\sin(\theta/2)$ with n and θ being the refractive index of the scattering medium and the scattering angle, respectively. For polydisperse particles, $g^{(1)}(q,\tau)$ takes the form

$$g^{(1)}(q,\tau) = \sum_i A_i e^{-D_i q^2 \tau}, \tag{2}$$

where A_i represents the scattering amplitude of the particle i with diffusion coefficient D_i. A regularization method (CONTIN [54,55]) was employed in analyzing the experimental data to solve Eq. (2) through eigenvalue decomposition combined with a smoothing technique, in order to obtain the diffusion coefficients D_i. The size distribution was expressed in terms of the average hydrodynamic radius R_{Hi} by means of the Stokes-Einstein relationship $R_{Hi}=K_BT/6\pi\eta D_i$, where K_BT is the thermal energy and η the viscosity of the aqueous phase.

D. Electrophoretic mobility measurements

The electrophoretic measurements were carried out by using the laser Doppler electrophoresis technique. The mobility u of the diffusing aggregates was converted into a ζ-potential value using the Smoluchowski relation $\zeta = u\eta/\epsilon$, where ϵ and η are the permittivity and the viscosity of the solution, respectively [56].

E. Static light scattering

Light scattering from vesicles and vesicle aggregates can be described within the Rayleigh-Gans-Debye approximation [57] of classical light scattering. The scattered or excess intensity due to a suspension of colloidal particles (considered monodisperse) can be written as

$$\frac{KC_L}{R_\theta} = \frac{1}{M_w P(q\Delta r) + S(q\Delta R) V_s N_0 C_L}, \tag{3}$$

where the Rayleigh ratio R_θ is defined as the light scattered at angle θ in excess of that scattered by the pure solvent divided by the scattered incident light. In this expression, C_L is the particle weight concentration and M_w the molecular weight, V_s is the volume from which the scattered light is collected (scattering volume) and N_0 is the Avogadro number. The factor $P(q\Delta r)$ takes into account the effect of light interference within the same particle (Δr stands for the internal coordinates), and $S(q\Delta R)$ is the interparticle interference factor (ΔR being the center-of-mass coordinates). Finally, the optical constant K, for vertically polarized incident light, is defined as

$$K = \frac{(2\pi)^2 n^2}{\lambda^4 N_0}\left(\frac{dn}{dc}\right)^2 \tag{4}$$

with n and (dn/dC) being the refractive index of the solvent and the refractive index increment due to the suspended particles, respectively, and λ the wavelength of the incident light in vacuo.

Under proper assumptions, Eq. (3) can be approximated as

$$\frac{KC_L}{R_\theta} \simeq \frac{1}{M_w P(qd)} + 2A_2 C_L \tag{5}$$

which is commonly used to interpret the static light scattering spectrum (here d simply stands for a characteristic size of the particle). From Eq. (5), the weight-average molecular weight M_w of the scatterers and the second virial coefficient A_2 of the suspension can be determined.

The second virial coefficient A_2 is related to an integral characteristic of the intermolecular interactions between the scatterers that can be written (for a spherically symmetric interparticle potential) as

$$A_2 = -\frac{N_0}{2M_w^2}\int_0^\infty (e^{-U_2(r)/K_B T} - 1) 4\pi r^2 dr, \tag{6}$$

where U_2 is the two-particle potential energy [58]. The variation of A_2 with solution conditions yields valuable information on the underlying effective pair interactions between suspended particles. A positive second virial coefficient (in homogeneous systems) means repulsive interactions.

In order to cancel out the influence of M_w on A_2, the second virial coefficient can be expressed in dimensionless form as

$$B_2 = A_2 \frac{M_w^2}{N_0}\frac{1}{V} = -\frac{1}{2V}\int_0^\infty (e^{-U_2(r)/K_B T} - 1) 4\pi r^2 dr, \tag{7}$$

where $V = \frac{4\pi R^3}{3}$ is the volume of the aggregate, with R its average radius. If the interactions are limited to the exclusion from the volume occupied by one particle of other particles ("hard spheres potential"), $B_2 = 4$ [58]. Values higher than $B_2 = 4$ indicate stronger repulsions, while lower or negative values indicate attractive interactions between the particles in the suspension.

Unfortunately, in the present case, the form factor $P(qd)$ cannot be accurately determined and, consequently, the product $M_w P(qd)$ (the intercept of the Debye plots) cannot be separated into its factors. However, the quantity $M_w P(qd)$ can be considered as an effective molecular weight $M_{w\text{eff}}$ in calculating an "effective virial coefficient" $B_{2\text{eff}} = B_2[P(qd)]^2$ [i.e., replacing M_w with $M_{w\text{eff}} = M_w P(qd)$ in Eq. (7)]. Since $P(qd)$ is ≤ 1 by definition, and it tends to the unity for small particles, a large increase of $B_{2\text{eff}}$ over the value measured for the isolated liposomes, clearly indicate an increase of the repulsions, so that this quantity can be usefully employed to quantitatively characterize interaggregate interactions [Eq. (7)].

The particle form factor $P(qd)$ depends on the particle shape and on the product qd between the scattering vector q and the typical particle size d. Since $P(qd)$ is due to intraparticle interference effects, it is significantly different from unity only for particles whose size is comparable to the wavelength of the light employed, i.e., for particles larger than about 50 nm. For simple geometrical shapes, the form factor is easily obtained. Isolated liposomes can be modeled as hollow spheres and, in this case, the form factor $P(qd)$ is given by [59]

$$P(x) = \left(\frac{3}{x^3(1-\gamma)}[\sin(x) - \sin(\gamma x) - x\cos(x) + \gamma x \cos(\gamma x)]\right), \tag{8}$$

where $x = qR_{\text{ex}}$ and $\gamma = R_{\text{in}}/R_{\text{ex}}$, with R_{ex} and R_{in} the outer and inner radius of the vesicle, respectively. For a liposome with an outer radius of 30 nm and a bilayer thickness of 4 nm, Eq. (8) yields a value of about $P = 0.83$.

In our case, polyion-decorated liposome aggregates, from transmission electron microscope images (Fig. 10, see also the figures in Ref. [8]) appear as compact clusters, but quite irregular, also because of the polydispersity of the single liposome particles. While limiting expressions can be obtained for (statistical) fractal clusters, for such irregular aggregates, an analytical form of the factor $P(qd)$ does not exist. Simulations [60] only provide the qualitative hint that the scattering of random aggregates of n monomers (spherical monomers) increases with n, but less than expected (a dependence

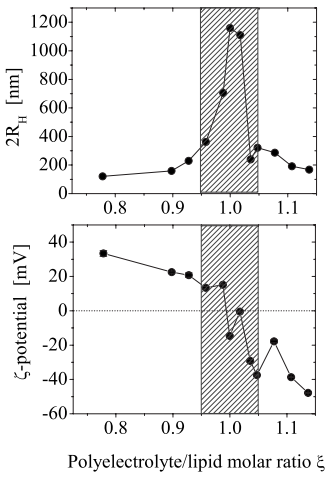

FIG. 1. Upper panel: The hydrodynamic diameter $2R_H$ of polyion-decorated liposome aggregates as a function of the polyelectrolyte/lipid monomolar ratio ξ, close to the isoelectric condition. Bottom panel: The ζ potential of the polyion decorated liposome aggregates as a function of the polyelectrolyte/lipid monomolar ratio ξ. The underlined regions mark the polyion concentrations to which the isoelectric condition takes place. This plot summarizes the two main effects, the reentrant condensation (upper panel) and the charge inversion (bottom panel), that characterize this class of colloid systems, under the balance of short-range attractive and long-range repulsive interactions.

on n^2) if there were no intra-aggregate interferences. This reduction in the scattering intensity decreases at the highest angles.

Also the impossibility of calculating the form factor from the geometry of the aggregates prevents the possibility of separating the effects due to the molecular weight M_w from those due the shape and size of the diffusing aggregate. Hence, in our analysis, the term $M_wP(qd)$, in Eq. (5), will be considered as an effective molecular weight M_{weff}.

III. RESULTS AND DISCUSSION

Figure 1 shows the typical aggregation behavior of this colloidal system. The average size and the ζ-potential value of the aggregates of pd-liposomes display, as a function of the polyelectrolyte/liposome charge ratio ξ, the typical effects of the reentrant condensation and of the charge inversion. In this case, liposomes are built up by cationic lipids, DOTAP, and the aggregation induced by a polyanion, poly(acrylate) sodium salt (NaPA). The charge ratio ξ is defined as the ratio of the total charge on the polyion chain in the solution to the total charge on the lipid. The charge inversion occurs at $\xi \simeq 1$ and close to this point, the aggregates become larger and larger.

This behavior has been investigated in detail, and we reported on this complex phenomenology in a series of recent works [8,11,21], where a comprehensive description of the whole process can be found. Here, we will focus on a further interesting effect, i.e., the large increase of the repulsion between the aggregates that occurs close to the isoelectric point.

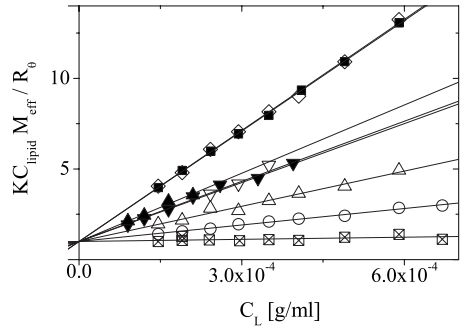

FIG. 2. Debye plot of polyion-decorated liposome aggregates. The ratio KC_LM_{weff}/R_θ is shown as a function of the liposome concentration C_L for different values of the polyelectrolyte/lipid molar ratio ξ below (empty symbols) and above (full symbols) the isoelectric point. The constant behavior observed for the liposomes without the added polyelectrolyte is also shown for comparison. ☒: liposomes; ○: ξ=0.56; △: ξ=0.70; ▽: ξ=0.85; ◇: ξ=0.99 (below the isoelectric point). ■: ξ=1.08; ▼: ξ=1.17; ▲: ξ=1.26 (above the isoelectric point). Closer and closer to the isoelectric point, the effective virial coefficient B_{2eff} increases, indicating a large increase of repulsion close to the point of charge inversion.

We will consider two different aqueous solution media, in the absence of added salt and in the presence of added NaCl salt, at two different concentrations (0.05 and 0.1 Mol/l). Although the phenomenology is rather similar, we will treat the two cases separately.

A. In the absence of added salt

Typical Debye plots of the light scattering data as a function of the liposome concentration C_L are shown in Fig. 2, for selected values of the polyelectrolyte/liposome molar ratio ξ, below, very close and above the point of charge inversion. Each sample, prepared at a fixed initial liposome concentration (C_L=0.6 mg/ml), was progressively diluted and the excess Rayleigh ratio R_θ measured.

As can be seen in Fig. 2, with the increase of the polyion to lipid ratio ξ (i.e., with the increase of the polyion concentration C), the slope of the curve KC_LM_{weff}/R_θ vs C_L rapidly becomes steeper and steeper, reaches a maximum for samples which are very close to the charge inversion point and then decreases again towards the initial values.

One might wonder if the iterated dilution of the liposome suspension, necessary for the construction of the Debye plot for each sample, could induce a spurious structural rearrangement of the aggregates. To answer to this question, in Fig. 3, we show for selected samples the average size of the aggregates, derived from dynamic light scattering measurements, at the different dilutions employed to build up the corresponding Debye plots shown in Fig. 2.

As can be seen, there is a substantial constancy, within the experimental errors, of the average size of the aggregate, which depends on the polyion/liposome molar ratio ξ in the usual manner (compare Figs. 1 and 2). This behavior was observed for all the samples investigated. The values of the hydrodynamic radii R_H shown in Fig. 3 are calculated from the diffusion coefficient D obtained from dynamic light scat-

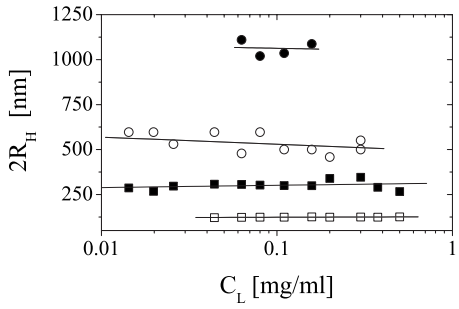

FIG. 3. The plot shows the constancy of the average size $2R_H$ of the polyion-decorated liposome aggregates as a function of the liposome concentration C_L during the dilution procedure employed in the measurement of the quantity KC_LM_{weff}/R_θ. The different average sizes refer to different polyelectrolyte/lipid molar ratios □: ξ=0.8; ○: ξ=1.0; •: ξ=1.05; ■: ξ=1.2.

tering, through the Stokes-Einstein relation, as $R_H=\frac{K_BT}{6D\pi\eta}$. For interacting particles, the measured diffusion coefficient D is expected to change with the volume fraction Φ of the dispersed objects as $D(\Phi)=D_0(1+\lambda\Phi)$ [61]. However, for charged colloidal particles and for $R\gg\kappa^{-1}$, the coefficient λ is of the order of 10 [62]. As a consequence, at the low volume fractions employed in this work (Φ varies from $\sim 3\times 10^{-4}$ to ~ 0.01), the expected changes of $D(\Phi)$ with the liposome concentration is too small to be appreciated. The constancy of the size of the aggregates evidenced in Fig. 3 rules out a restructuring of the aggregates upon the dilution procedure required for the Debye plots.

In Fig. 4, the second virial coefficient A_2, obtained from the Debye plots, is shown as a function of the polyelectrolyte/lipid molar ratio ξ. From its definition [Eq. (6)], the quantity A_2 depends on the interactions between the suspended particles but also on their molecular weight.

However, when the explicit dependence of the virial coefficient on the molecular weight is eliminated and the coefficient is rewritten in its dimensionless form $B_{2\text{eff}}$ [see Eq. (7)], when this quantity is plotted vs the polyelectrolyte/liposome molar ratio ξ, a sharp maximum clearly appears in correspondence of the isoelectric condition (Fig. 5). This sharp increase of the virial coefficient $B_{2\text{eff}}$ indicates that repulsive inter-aggregate interactions rapidly become very large when the size of the aggregates formed by the pd-liposomes increases toward its maximum at the isoelectric point.

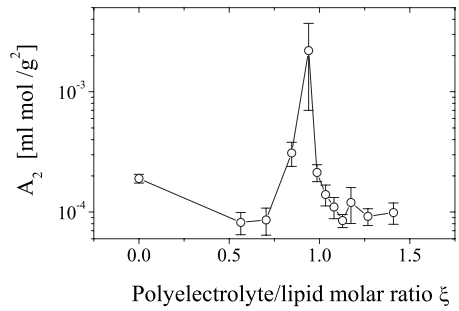

FIG. 4. The second virial coefficient A_2 deduced from the Debye plots as a function of ξ, in the absence of added salt.

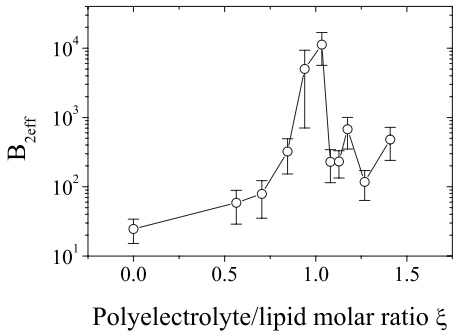

FIG. 5. The dimensionless second virial coefficient $B_{2\text{eff}}$, as a function of ξ. The coefficient $B_{2\text{eff}}$ is calculated by means of Eq. (7) from the values of A_2 and M_{weff} obtained from the Debye plots and the values of the hydrodynamic radius measured by means of dynamic light scattering.

B. In the presence of added salt

In the presence of added simple salt (NaCl), the aggregation phenomenology is rather more complex, since in the vicinity of charge inversion, a region of instability appears and the aggregates form larger and larger clusters, up to a complete flocculation in a long time regime. Moreover, in a region around the isoelectric point, whose extension widens with the salt concentration, the scattered light correlation functions deviate from a single exponential decay and bimodal distributions appear. We have investigated this peculiar behavior in a previous work, to which we refer to for a detailed phenomenological description of this process [11].

A typical behavior is shown in Fig. 6, where we compare the increase of the average radius $\langle R/R_0\rangle$ of the pd-liposome aggregates (normalized by the primary particle radius R_0) as a function of the polyelectrolyte lipid molar ratio ξ, in the presence of added salt (at two different concentrations C_s=0.05 mol/l and C_s=0.1 mol/l) and in absence of added salt.

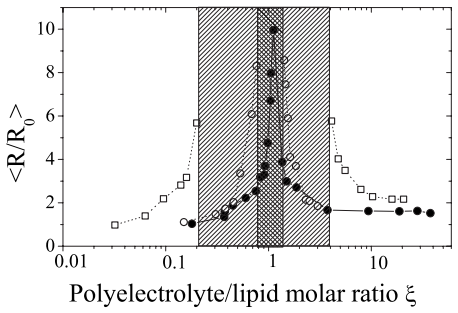

FIG. 6. Average radius $\langle R/R_0\rangle$ of polyion-decorated liposome clusters as a function of the polyelectrolyte/lipid molar ratio ξ, in the presence of different amounts of simple electrolyte (NaCl): □: 0.1 mol/l; ○: 0.05 mol/l. In all samples, the molecular weight of the polyion was 60 kD. For comparison, results obtained in the absence of added salt (•) are also shown. The shaded regions mark boundaries of polyion concentration ranges where the DLS correlation functions display two characteristic decay times. These regions widen with the increase of the salt concentration.

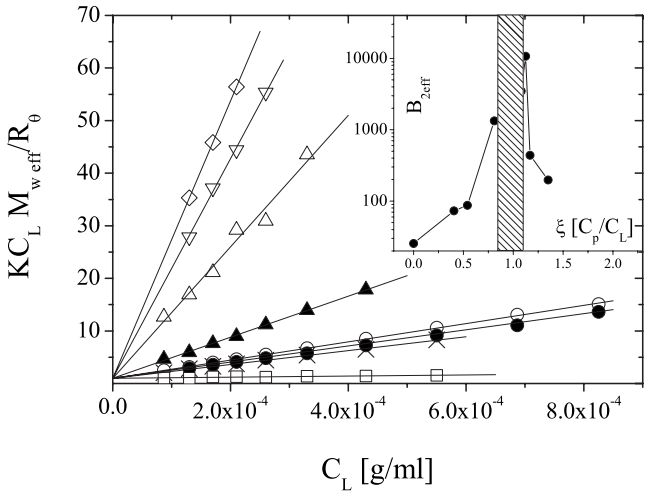

FIG. 7. Debye plot of polyion decorated liposome aggregates in the presence of added salt (0.05 mol/l NaCl). The ratio RC_LM_{weff}/R_θ is shown as a function of the liposome concentration C_L for different values of the polyion/lipid molar ratio ξ. □: ξ=0 (single liposomes, no polyelectrolyte added); ×: ξ=0.40; ○: ξ=0.54; △: ξ=0.81; ▽: ξ=1.08; ◇: ξ=1.12; ▲: ξ=1.17; ●: ξ=1.35. Full lines represent a linear fit of the data. The inset shows the normalized second virial coefficient B_{2eff}, deduced from the Debye plots. The shaded region marks the polyion concentration region very close to the isoelectric point, where the DLS correlation functions display two characteristic decay times (see text).

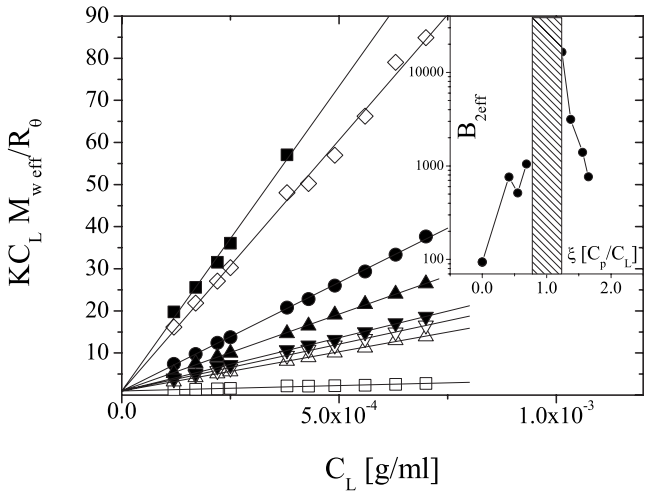

FIG. 8. Debye plot of polyion decorated liposome aggregates in the presence of added salt (0.1 mol/l NaCl). The ratio RC_LM_{weff}/R_θ is shown as a function of the liposome concentration C_L for different values of the polyion/lipid molar ratio ξ. □: ξ=0 (single liposomes, no polyelectrolyte added); △: ξ=0.41; ▽: ξ=0.55; ◇: ξ=0.69; ■: ξ=1.29; ●: ξ=1.37; ▲: ξ=1.56; ▼: ξ=1.65. Full lines represent a linear fit of the data. The inset shows the normalized second virial coefficient B_{2eff}, deduced from the Debye plots. The shaded region marks the polyion concentration region very close to the isoelectric point, where the DLS correlation functions display two characteristic decay times (see text).

An analysis of the scattered light correlation functions of aggregates very close to the isoelectric point (shaded regions in Fig. 6) results in bimodal distributions of relaxation times. Moreover, in this region the suspension is not stable and often flocculates, with characteristic times that are not completely reproducible. For this reason, in our analysis, we did not consider samples inside this regions any further.

However, outside this region, but sufficiently close to the isoelectric condition, the phenomenology described above in the absence of salt, i.e., an increase of repulsive interactions in vicinity of the isoelectric condition, is also observed in the presence of added salt, as shown in Figs. 7 and 8, for the two salt concentrations investigated 0.05 and 0.1 M NaCl.

C. The charge of the aggregates at the isoelectric point

Charged colloidal particles are usually stabilized by strong electrostatic repulsion and, also in the case of suspensions of highly charged liposomes, the stabilization is of electrostatic nature. In fact, above a critical value of the ionic strength of the solution, liposomes begin to aggregate and the suspension eventually flocculate, following the usual Derjaguin-Landau-Verwey-Overbeek (DLVO) behavior [22]. Moreover, the measured structure factor for such systems can be satisfactorily calculated hypothesizing a repulsive interaction between the liposomes described as a simple screened Coulomb potential [63].

A similar behavior has been also observed for pd-liposome aggregates in the presence of large polyelectrolyte excess. A significant aggregation and flocculation of a DOTAP liposome suspension, prepared at the typical volume fractions employed in this work, is easily obtained both by adding NaCl at concentrations of the order of 0.5 M and by adding NaPA at a similar monomolar concentration [22]. Such monomolar concentrations of (NaPA) correspond to values of the charge ratio ξ close to 50–100. The reentrant condensation described above and observed in a range of ξ close to the point of charge inversion (in the vicinity of $\xi \simeq 1$) is a completely different phenomenon. Moreover, the reentrant condensation shows a marked dependence on the molecular weight of the polyelectrolyte employed to induce the aggregation [20], suggesting that the nonhomogeneous distribution of the adsorbed polyions at the liposome surface plays an essential role in the aggregation process.

To justify, at least qualitatively, the formation of large stable strongly interacting aggregates observed in these systems close to the point of charge inversion, we address to a potential of mean force between two spheroidal colloidal particles recently proposed by Velegol and Thwar [46]. These authors have developed an extension of the classical DLVO theory taking into account the effect of a nonuniform surface charge distribution on the potential between two approaching particles, on the basis of the Hogg-Healy-Fuerstenau model [64]. The nonuniformity in the charge distribution, that in this case is originated by the correlated adsorption of polyions onto the liposome surface, imparts to the system the attractive contribution, allowing colloidal aggregation. Within this model, the average potential of interaction between two nonuniformly charged colloidal spheres can be written as

$$\langle \Phi_{VT}(d) \rangle = \pi\varepsilon \frac{R_A R_B}{R_A + R_B} \left[(\zeta_A^2 + \zeta_B^2 + \sigma_A^2 + \sigma_B^2) \ln(1 - e^{-2\kappa d}) + 2\zeta_A \zeta_B \ln\left(\frac{1 + e^{-\kappa d}}{1 - e^{-\kappa d}} \right) \right] \quad (9)$$

In this expression, ε is the dielectric permittivity of the dispersing medium, d is the distance between the surfaces of the two particles with radii R_A and R_B, respectively, k is the inverse of the Debye screening length and ζ_i and σ_i $(i=A,B)$ are the mean value of the ζ potential (averaged twice, on the whole surface of the particle, and ensemble averaged on type i particles) and its standard deviation.

This potential combines a repulsive monopole term and an attractive interaction that arises from the nonuniform distribution of charge on the particles. From Eq. (9), it results that, in the presence of a charge nonuniformity $(\sigma_i \neq 0)$, also in the case of two particles bearing a net charge of the same sign, an attractive component is always present, since the first term in the parenthesis [Eq. (9)] is always negative. The repulsive part (in the case of similarly charged particles), represented by the term which is proportional to the $\zeta_A \zeta_B$ product, cancels out when the net charge on the particles is zero.

In the case of pd-decorated liposomes, the correlated adsorption of the polyelectrolytes is the origin of a certain degree of nonuniformity of the surface charge distribution $(\sigma \neq 0)$. This nonuniform distribution is responsible of an attractive interaction term ("charge patch attraction" [44–46]). This nonuniformity of the distribution of the adsorbed macroions (polyelectrolytes) at the liposome surface clearly depend on their size and charge (a simple monovalent electrolyte would spread almost uniformly, except for the finite dimension of the ions). This circumstance justifies the dependence of the efficiency of the aggregation process on the degree of polymerization of the polyelectrolyte. Obviously, the residual net charge on the particles, due to the incomplete neutralization of the liposomes (at the lower polyelectrolyte/liposome ratios ξ) or to the overcharging (at higher ξ), would contribute a net repulsion on both sides of the charge neutralization point, resulting in the reentrant condensation.

At medium to high values of the ionic strength of the solution, where the electrostatic interactions are more effectively screened, dispersion forces become comparatively important. To this end, to take into account van der Waals interactions between the aggregates a term [65]

$$\Phi_{vdW}(d) = -\frac{A R_A R_B}{6(R_A + R_B)} \left(\frac{1}{d + h_A + h_B} - \frac{1}{d + h_A} - \frac{1}{d + h_B} + \frac{1}{d} \right) - \frac{A}{6} \ln\left[\frac{d(d + h_A + h_B)}{(d + h_A)(d + h_B)} \right] \quad (10)$$

can be added to the potential [Eq. (9)]. This expression, derived for shelled spheres (with radius R_A and R_B and shell thickness h_A and h_B, respectively), is appropriate for liposomes and liposome aggregates where the presence of the water core substantially decreases the van der Waals attraction.

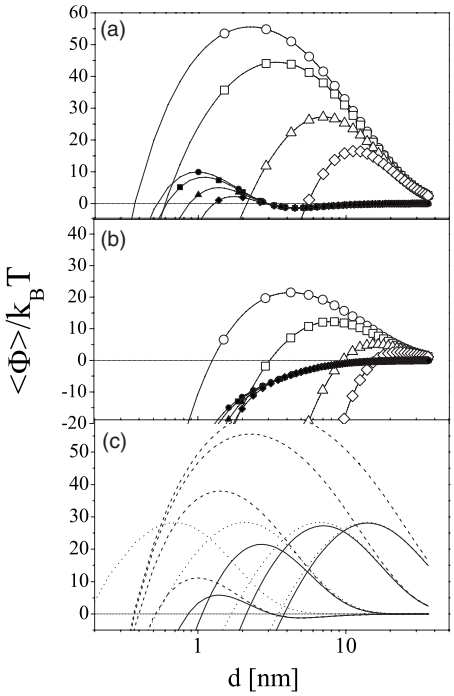

FIG. 9. The potential of mean force between two identical spherical particles as a function of the distance d between their surfaces. The potential is plotted in units of the thermal energy $K_B T$ at room temperature (25 °C). The curves are calculated for different choices of the electrical parameters ζ and σ and k^{-1}, and for different values of the particle radius. (a) $R=250$ nm, $\zeta=20$ mV. Open symbols: $k^{-1}=9.6$ nm (10^{-3} M NaCl); Closed symbols: $k^{-1}=0.96$ nm (10^{-1} M NaCl). (Circle): $\sigma=0$ mV; (square): $\sigma=10$ mV; (triangle): $\sigma=20$ mV; (lozenge): $\sigma=30$ mV. (b) $R=500$ nm, $\zeta=10$ mV. Open symbols: $k^{-1}=9.6$ nm (10^{-3} M NaCl); closed symbols: $k^{-1}=0.96$ nm (10^{-1} M NaCl). (Circle): $\sigma=0$ mV; (square): $\sigma=10$ mV; (triangle): $\sigma=20$ mV; (lozenge): $\sigma=30$ mV. (c) solid lines: the total potential $\Phi(d)=\Phi_{VT}(d)+\Phi_{wdW}(d)$; dotted lines: the Velegol potential $\Phi_{VT}(d)$; dashed lines: the DLVO potential Φ_{DLVO}. The curves have been calculated for the following values of the screening length $k^{-1}=1$, 3 10, 20 nm and, correspondingly, the curves shift from left to right.

Figure 9 shows an example of the behavior of the potential of mean force $\Phi(d)=\Phi_{VT}(d)+\Phi_{vdW}(d)$ between two identical particles of radius R, for different values of the electrical parameters ζ and σ and different values of the ionic strength of the solution.

For smaller particles [Fig. 9(a), $R=250$ nm] and at a reduced ionic strength (open symbols), the potential barrier to the aggregation decreases its height with the increasing of the surface charge nonuniformity, moving toward higher distances between the particles.

The two series of curves refer at two different screening lengths $\kappa^{-1}=9.6$ nm and $\kappa^{-1}=0.96$ nm and correspond to a 0.1 and 0.001 molar concentration of a 1:1 electrolyte.

In the absence of added simple salt, at the lipid/polyelectrolyte concentration employed in this work, the lowest concentration (0.001 M) can be considered a superior limit for the concentration of the free counterions in the solution [66] (Na^+ ions derived from the polyelectrolyte and

Cl^- ions from the cationic lipid). At the highest ionic strength, the potential barrier is strongly reduced (solid symbols), due to the effective screening of the electrostatic repulsion.

Moreover, for larger particles and a smaller value of the ζ potential (closer to the charge inversion point), Fig. 9(b) shows that, at the higher ionic strength (solid symbols), the potential is always attractive and a sample in these conditions would flocculate. At lower ionic strength, however, (open symbols) the potential barrier is still present.

In Figs. 9(a) and 9(b), the curves for $\sigma=0$ represent the behavior of a typical DLVO potential

$$\Phi_{\mathrm{DLVO}}(d) = \Phi_{\mathrm{vdW}}(d) + \Phi_{\mathrm{VT}}(d)_{\sigma=0} \tag{11}$$

since, in this case, expression (9) reduces to the typical form of the electrostatic repulsion between two spherical particles employed in DLVO theory [46,61]. As Fig. 9(c) shows, the main contribution of the charge nonuniformity, in addition to contributing an obvious reduction of the potential barrier height, is the significant shift of the position of the barrier maximum at larger interparticle distances, an effect that is comparatively larger at lower ionic strengths. The stability of larger and larger aggregates close to the point of charge inversion is an effect of the presence of the potential barrier. The presence of the nonuniform charge distribution at the liposome surface increases the range where interactions occur, which shifts towards larger distance.

The height H of this potential barrier is roughly proportional to the radius of the colliding particles multiplied by the square of the ζ potential $H \propto R\zeta^2$. As a consequence, at each finite temperature, and at constant values of ζ potential (i.e., at a fixed charge ratio ξ), the probability that a collision of two large aggregates results in their sticking together decreases as the size of the colliding particles increases.

At an intuitive level, this dependence of the interaction on the size of the particles can be justified by the following argument. The interaction described by the potential in Eq. (9) is ultimately due to the overlapping of the diffuse layers of the two approaching particles. Assuming (as is usually the case for aqueous solvents) that the diffuse layer thickness κ^{-1} is much smaller than the particle radius (in the present case this assumption, with primary particles that have a radius $\gtrapprox 30$ nm is reasonable), the particle interaction can be described in a quasiplanar geometry (Derjaguin approximation [67]). However, the effective contact area is larger and larger when the size of the approaching particles increases. Moreover, as primary particles, liposomes are easily deformable and, as is apparent from the TEM images shown in Fig. 10, they reshape within the aggregate, flattening at the contact sites (and this fact could also contribute to increase the strength of the interactions, see, for example Ref. [68]). The whole aggregate continues to appear roundish in shape, but delimited by surfaces with a much larger curvature radius than the primary component liposomes.

As a consequence of the dependence of the two-particle potential on the particle size, the cluster-cluster aggregation process would practically end when the aggregates reach a size for which the potential barrier height is several K_BT. In other words, within this picture, the clusters would rather be kinetically stabilized than be true equilibrium aggregates, but with a mechanism which is different from the one usually assumed, where kinetic stabilization is ascribed to the progressive reduction of the mobility of the larger aggregates.

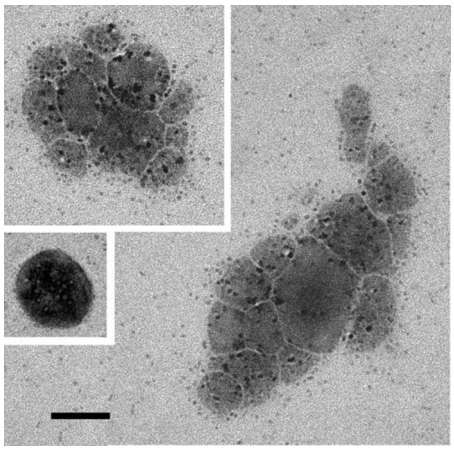

FIG. 10. Transmission electron microscopy images of typical pd-liposome aggregates. Isolated pd-liposomes (small inset) appear almost spherical. Conversely, within the aggregates, the liposomes appear flattened at the contact sites and close packed together. The whole aggregates maintain a roundish shape, but are delimited by surfaces with a larger curvature radius than the primary component liposomes. Bar represents 100 nm. The samples shown are not stained, the contrast observed is obtained by preparing the liposomes with a proper concentration of CsCl in the aqueous core, with a procedure which is described in detail in Ref. [8].

Within this picture, the counterintuitive increase of the repulsive interaction observed close to the point of charge inversion, where the ζ-potential goes to zero, also finds a plausible justification. In fact, as it has been already pointed out, while close to the reversal point the ζ potential shows a linear behavior [69], the aggregate size diverges much more rapidly than linearly [20,69], so that the increase in the aggregate size overcompensates for the decrease of ζ potential. Consequently, the height of the potential barrier increases. Figure 11 (upper part) shows, in a log-log scale, the divergent behavior of the aggregate size close to the point of charge inversion. This behavior is well approximated with a power law with an exponent of the order of 4 (or, in any case, $\gtrsim 3$, see also Ref. [69]). In the same figure (lower part), the approximately linear behavior of the ζ potential in a range across the charge inversion point is also shown. For the example shown in Fig. 11, the increase of the barrier height as $\xi \to \xi_0$ could be evaluated approximately as $H \propto R\zeta^2 \sim (\xi - \xi_0)^{-2}$.

In summary, the whole process of the reentrant condensation could be described in the following terms. At increasing the polyelectrolyte/liposome ratio, the net charge of the pd-liposomes decreases at first in absolute value, changes its sign at the point of charge inversion and then increases again up to the maximum overcharging. Due to the correlated adsorption of the polyelectrolyte chains, the charge distribution at the pd-liposome surface is certainly nonuniform. The attractive term in the potential induces the aggregation of the pd-liposomes, but since the energy barrier to the collapse, for

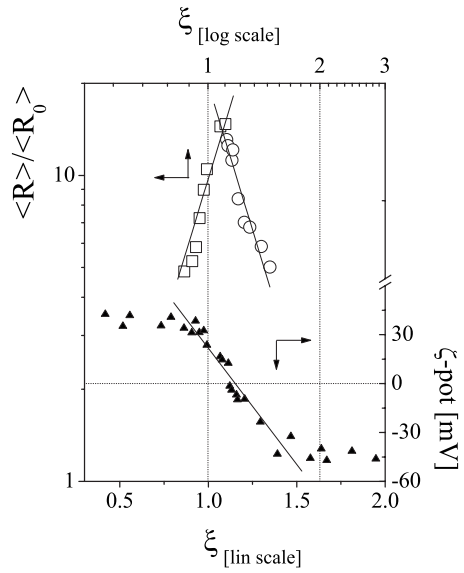

FIG. 11. Close to the isoelectric point the ζ-potential is approximately linear (lower part). However (upper part), in the same range of ξ, the size of the aggregates grows as ξ^n, with $m \simeq 4$. The upper log-scale and the lower linear-scale are drawn in such a way that the $\xi=1$ values coincide. In the figure the power laws superimposed to the measured radii have an exponent equal to ±4.

given average net charge and nonuniformity, increases with the size of the colliding particles, when the aggregates reaches a certain size, the probability that two colliding aggregates sticks upon collision becomes negligible and the aggregates stops growing. At any given polyelectrolyte/liposome ratio, a limiting radius is reached that is larger and larger as the net charge on the pd-liposomes (and consequently on the aggregates) decreases approaching the neutralization point. Crossing that point, the pd-liposomes are progressively more overcharged and the limiting radius decreases accordingly. On the other hand, for given values of the surface averaged ζ potential and of its variance, the energy barrier increases with the particle radius, so that close to the isoelectric condition, where larger aggregates form, the repulsive interactions, in terms of the virial coefficient, increase accordingly. An effect which contrasts with what would appear intuitive, that repulsion would diminish when the net charge on the aggregates goes to zero.

IV. CONCLUSIONS

We have studied the aggregation of charged mesoscopic colloidal particles induced by oppositely charged linear polyions by means of a combined use of dynamic and static light scattering measurements. We employed charged vesicles built up by a cationic lipid, DOTAP, and a simple linear flexible polyion, poly(acrylate) sodium salt. This system has been extensively studied and the main peculiar characteristics have been well assessed as far as structural and dynamical properties are concerned. Here, we have extended our previous measurements, investigating in deeper details the region of the phase diagram of this system very close to the charge inversion condition, where large equilibrium clusters are formed. Both in the absence and in the presence of added simple salt (that contributes to screen the electrostatic interactions), we found that the second virial coefficient, close to the charge inversion point, markedly increases over the value that this parameter assumes far from the isoelectric condition, both below (down to the bare liposomes) and above it (up to the overcharged isolated pd-liposomes). We derived the second virial coefficients from the slope of the linear dependence of the inverse of the Rayleigh ratio on the aggregate concentration. This increase is interpreted as due to increased repulsions between the aggregates close to the isoelectric point.

To explain this increase, a mechanism is hypothesized where the nonhomogeneity of the charge distribution at the pd-liposome surface, due to the correlated adsorption of the polyelectrolyte, plays a major role. Velegol and Thwar [46] have recently shown that a nonuniform charge distribution at the surface of colloidal particles gives place to an interparticle potential that, even in the case of same-sign charged particles, has an attractive component. Moreover, this potential, for some combinations of the values of the parameters involved (the surface averaged net charge of the particles and the variance of the surface charge distribution) shows a maximum, close to the particles surface, that may represent an energy barrier that hinders their sticking together. The height of this barrier apparently increases with the radius of curvature of the surface of the two approaching particles, i.e., with the size of the aggregates, in the case of the very deformable pd-liposomes and depends on the particle ζ potential, going approximately as $H \propto R\zeta^2$. By adding to this potential a contribution from van der Waals attraction, which acts at smaller distance, this picture does not result substantially modified.

After all, the above stated mechanism would also allow to explain two characteristics of the aggregation in these systems that are difficult to harmonize within the usual DLCA picture, i.e., the narrow size distribution of the aggregates, and the elongated aspect that larger aggregates assume. In fact, because of collisions of two large particles, the height of the barrier rapidly becomes insurmountable, a single pd-liposome still has some probability of sticking to a much larger aggregate, since the barrier height is roughly proportional to the contact area and this quantity is limited by the surface of the smallest of the two colliding particles. Such a "selection rule" in the sticking mechanism would presumably yield a size distribution of the aggregates with a narrow peak at the large size end. On the contrary, with the usual assumption of DLCA aggregation, that larger clusters stick more easily together but the probability of their collisions is low due to their reduced mobility, a broad size distribution is expected. Moreover, being governed by the local radius of curvature, the sticking probability will be larger for zones of the aggregates where they present bulges or protuberances, so that larger aggregates will tend to grow assuming elongated shapes.

Although the overall phenomenology is similar to the one observed in other systems, where the long-range repulsion is attributable to screened electrostatic interactions and the attraction to short-range potentials of different nature (deple-

tion interactions or van der Waals forces, for example), the pd-liposome system presents peculiar characteristics. In this case, both the attractive and the repulsive interactions apparently share a common electrostatic nature.

While there is an increasing evidence that the attractive part of the potential arises from the correlated adsorption of the polyelectrolyte chains at the liposome surface, a satisfactory description of the whole mechanism of aggregation is still far to be completed. Different hypotheses have been put forward in an attempt to consider the different aspects of the complex phenomenology observed. Although the mechanism hypothesized in this work is able to take into account several of those aspects, it may be somewhat speculative at the level of our present knowledge of the system. More studies are required to investigate in details the mechanisms for forming different cluster regimes and to clarify how the ranges of attraction and repulsion could affect the characteristic size of the clusters and their overall electric charge.

ACKNOWLEDGMENTS

S.S. gratefully acknowledges the financial support of CNR-INFM CRS-SOFT.

[1] T. Nylander, Y. Samoshina, and B. Lindman, Adv. Colloid Interface Sci. **123-126**, 105123 (2006).
[2] D. Ferber, Science **294**, 1638 (2001).
[3] M. Pedroso De Lima, S. Simoes, P. Pires, H. Faneca, and N. Duzgunes, Adv. Drug Delivery Rev. **47**, 277 (2001).
[4] M. C. Woodle and P. Scaria, Curr. Opin. Colloid Interface Sci. **6**, 77 (2001).
[5] C. R. Safinya, Curr. Opin. Struct. Biol. **11**, 440 (2001).
[6] I. Koltover, T. Salditt, and C. R. Safinya, Biophys. J. **77**, 915 (1999).
[7] J.O. Rädler, I. Koltover, T. Salditt, and C. R. Safinya, Science **275**, 810 (1997).
[8] F. Bordi, C. Cametti, S. Sennato, and M. Diociaiuti, Biophys. J. **91**, 1513 (2006).
[9] R. Sanchez and P. Bartlett, J. Phys.: Condens. Matter **17**, S3551 (2005).
[10] F. Sciortino, P. Tartaglia, and E. Zaccarelli, J. Phys. Chem. B **109**, 21942 (2005).
[11] F. Bordi, C. Cametti, M. Diociaiuti, and S. Sennato, Phys. Rev. E **71**, 050401(R) (2005).
[12] A. Stradner, H. Sedgwick, F. Cardinaux, W. C. K. Poon, S. U. Egelhaaf, and P. Schurtenberger, Nature (London) **432**, 492495 (2004).
[13] S. U. Sedgwick, H. Egelhaaf, and W. C. K. Poon, J. Phys.: Condens. Matter **16**, S4913 (2004).
[14] H. Sedgwick, K. Kroy, A. Salonen, M. Robertson, S. Egelhaaf, and W. Poon, Eur. Phys. J. E **16**, 7780 (2005).
[15] A. I. Campbell, V. J. Anderson, J. S. van Duijneveldt, and P. Bartlett, Phys. Rev. Lett. **94**, 208301 (2005).
[16] J. Groenewold and W. K. Kegel, J. Phys. Chem. B **105**, 11702 (2001).
[17] S. Mossa, F. Sciortino, E. Zaccarelli, and P. Tartaglia, Langmuir **20**, 10756 (2004).
[18] C. B. Muratov, Phys. Rev. E **66**, 066108 (2002).
[19] R. P. Sear, S.-W. Chung, G. Markovich, W. M. Gelbart, and J. R. Heath, Phys. Rev. E **59**, R6255 (1999).
[20] F. Bordi, C. Cametti, M. Diociaiuti, D. Gaudino, T. Gili, and S. Sennato, Langmuir **20**, 5214 (2004).
[21] S. Sennato, F. Bordi, C. Cametti, M. Diociaiuti, and M. Malaspina, Biochim. Biophys. Acta **1714**, 11–24 (2005).
[22] B. F. Sennato, and S. Cametti, Europhys. Lett. **68**, 296 (2004).
[23] E. Gonalves, R. J. Debs, and T. D. Heath, Biophys. J. **86**, 1554 (2004).
[24] J. Piedade, M. Mano, M. Pedroso De Lima, T. Oretskaya, and A. Oliveira-Brett, Biosens. Bioelectron. **20**, 975984 (2004).
[25] L. Ciani, S. Ristori, A. Salvati, L. Calamai, and G. Martini, Biochim. Biophys. Acta **1664**, 70 (2004).
[26] A. Y. Grosberg, T. T. Nguyen, and B. I. Shklovskii, Rev. Mod. Phys. **74**, 329 (2002).
[27] J. Mou, D. M. Czajkowsky, Y. Zhang, and Z. Shao, FEBS Lett. **371**, 279 (1995).
[28] Y. Fang and J. Yang, J. Phys. Chem. B **101**, 441 (1997).
[29] H. Clausen-Schaumann and H. E. Gaub, Langmuir **15**, 8246 (1999).
[30] T. T. Nguyen, A. Y. Grosberg, and B. I. Shklovskii, Phys. Rev. Lett. **85**, 1568 (2000).
[31] M. Tanaka and Y. Grosberg, J. Chem. Phys. **115**, 567 (2001).
[32] J.-F. Berret, J. Chem. Phys. **123**, 164703 (2005).
[33] A. E. Larsen and D. G. Grier, Nature (London) **385**, 230 (1997).
[34] J. C. Butler, T. Angelini, J. X. Tang, and G. C. L. Wong, Phys. Rev. Lett. **91**, 028301 (2003).
[35] G. C. L. Wong, A. Lin, J. X. Tang, Y. Li, P. A. Janmey, and C. R. Safinya, Phys. Rev. Lett. **91**, 018103 (2003).
[36] Y. K. Leong, Colloid Polym. Sci. **279**, 82 (2001).
[37] W. H. Walker and S. B. Grant, Colloids Surf., A **119**, 229 (1996).
[38] N. Grønbech-Jensen, R. J. Mashl, R. F. Bruinsma, and W. M. Gelbart, Phys. Rev. Lett. **78**, 2477 (1997).
[39] J. Wu, D. Bratko, and J. M. Prausnitz, Proc. Natl. Acad. Sci. U.S.A. **95**, 15169 (1998).
[40] P. Linse and V. Lobaskin, Phys. Rev. Lett. **83**, 4208 (1999).
[41] R. Messina, C. Holm, and K. Kremer, Phys. Rev. Lett. **85**, 872 (2000).
[42] A. Najia and R. Netz, Eur. Phys. J. E **13**, 43 (2004).
[43] P. Linse, J. Phys.: Condens. Matter **14**, 13449 (2002).
[44] S. J. Miklavic, D. Y. C. Chan, L. R. White, and T. W. Healy, J. Phys. Chem. **98**, 9022 (1994).
[45] A. V. M. Khachatourian and A. O. Wistrom, J. Phys. Chem. B **102**, 2483 (1998).
[46] D. Velegol and P. K. Thwar, Langmuir **17**, 7687 (2001).
[47] P. N. Segre, V. Prasad, A. B. Schofield, and D. A. Weitz, Phys. Rev. Lett. **86**, 6042 (2001).
[48] A. Coniglio, L. De Arcangelis, E. Del Gado, A. Fierro, and N. Sator, J. Phys.: Condens. Matter **16**, S4831 (2004).
[49] F. Sciortino, S. Mossa, E. Zaccarelli, and P. Tartaglia, Phys.

Rev. Lett. **93**, 055701 (2004).
[50] G. F. Wang and S. K. Lai, Phys. Rev. Lett. **82**, 3645 (1999).
[51] A. Robert, E. Wandersman, E. Dubois, V. Dupuis, and R. Perzynski, Europhys. Lett. **75**, 764 (2006).
[52] B. J. Berne and R. Pecora, *Dynamic Light Scattering* (Dover, New York, 2000).
[53] V. Degiorgio and J. B. Lastovka, Phys. Rev. A **4**, 2033 (1971).
[54] S. Provencher, Comput. Phys. Commun. **27**, 213 (1982).
[55] S. Provencher, Comput. Phys. Commun. **27**, 229 (1982).
[56] A. V. Delgado, F. Gonzlez-Caballero, R. J. Hunter, L. K. Koopal, and J. Lyklema, Pure Appl. Chem. **77**, 1753 (2005).
[57] J. K. G. Dhont, *An Introduction to Dynamics of Colloids, Studies in Interface Science* (Elsevier, Amsterdam, 1996).
[58] D. A. McQuarrie, *Statistical Mechanics*, 2nd ed. (University Science Books, Sausalito, CA, 2000).
[59] A. K. Mukherjee, K. S. Schmitz, and L. B. Bhuiyan, Langmuir **18**, 4210 (2002).
[60] V. A. Bloomfield, Biopolymers **54**, 168 (2000).
[61] B. U. Felderhof, J. Phys. A **11**, 929 (1978).
[62] D. N. Denkov and D. N. Petsev, Physica A **183**, 462 (1992).
[63] C. Haro-Pérez, M. Quesada-Pérez, J. Callejas-Fernández, E. Casals, J. Estelrich, and R. Hidalgo-Álvarez, J. Chem. Phys. **118**, 5167 (2003).
[64] R. Hogg, T. W. Healy, and D. Fuersstenau, Trans. Faraday Soc. **62**, 1638 (1966).
[65] R. Tadmor, J. Phys.: Condens. Matter **13**, L195 (2001).
[66] K. Kamburova and T. Radeva, J. Colloid Interface Sci. **313**, 398 (2007).
[67] B. V. Derjaguin and L. Landau, Acta Physicochim. URSS **14**, 633 (1941).
[68] D. N. Petsev, Langmuir **15**, 1096 (1999).
[69] F. Bordi, C. Cametti, C. Marianecci, and S. Sennato, J. Phys.: Condens. Matter **17**, S3423 (2005).